Alterations in enterohepatic Fgf15 signaling and changes in bile acid composition depend on localization of murine intestinal inflammation

Rau, Monika ; Stieger, Bruno ; Monte, Maria J ; Schmitt, Johannes ; Jahn, Daniel ; Frey-Wagner, Isabelle ; Raselli, Tina ; Marin, Jose J G ; Müllhaupt, Beat ; Rogler, Gerhard ; Geier, Andreas

Abstract: BACKGROUND: Fibroblast growth factor (FGF) 15/19 is part of the gut-liver crosstalk accounting for bile acid (BA) metabolism regulation. Dysregulation of fibroblast growth factor 15/19 signaling is observed in different pathological conditions, for example, in gastrointestinal diseases such as inflammatory bowel disease (IBD). To understand the molecular bases, we analyzed the enterohepatic regulation of Fgf15-mediated pathway in 2 different inflammatory bowel disease mouse models. METHODS: Target genes of the BA-farnesoid-X-receptor (Fxr)-Ffg15 axis were quantified by RT-PCR or western blotting in gut and liver of dextran sulfate sodium (DSS)-treated and IL10 mice. Serum Fgf15 levels were analyzed by ELISA. Biliary and fecal BA composition was differentiated by HPLC-MS/MS. RESULTS: Dextran sulfate sodium-treated mice with ileum-sparing colitis showed higher Fgf15 serum levels. In contrast, IL10 mice with ileitis had a trend toward decreased Fgf15 serum levels compared with controls and increased expression of Asbt as a negative Fxr-target gene. In hepatic tissue of both models, no histological changes, but higher interleukin 6 (IL-6) mRNA expression and down-regulation of Fxr and Cytochrom P450 7a1 mRNA expression were observed. Fibroblast growth factor receptor 4 up-regulation was in line with higher Fgf15 serum levels in dextran sulfate sodium-treated mice. A distinct fecal BA profile was observed in both models with significantly higher levels of taurine-conjugated BA in particular tauro- -muricholic acid in IL10 mice. CONCLUSIONS: Ileum-sparing colitis is characterized by activation of Fxr-Fgf15 signaling with higher expression of Fxr-target gene Fgf15, whereas ileal inflammation showed no signs of Fxr-Fgf15 activation. Abundance of BA such as T- -MCA may be important for intestinal Fxr activation in mice.

DOI: https://doi.org/10.1097/MIB.0000000000000879

Alterations in Enterohepatic Fgfl5 Signaling and Changes in Bile Acid Composition Depend on Localization of Murine Intestinal Inflammation

Monika Rau, MD, Bruno Stieger, PhD,† Maria J. Monte, PhD,‡ Johannes Schmitt, PhD,* Daniel Jahn, PhD,* Isabelle Frey-Wagner, PhD,§ Tina Raselli,§ Jose J. G. Marin, PhD,‡ Beat Müllhaupt, MD,§ Gerhard Rogler, MD, PhD,§ and Andreas Geier, MD*,§*

Background: Fibroblast growth factor (FGF) 15/19 is part of the gut-liver crosstalk accounting for bile acid (BA) metabolism regulation. Dysregulation of fibroblast growth factor 15/19 signaling is observed in different pathological conditions, for example, in gastrointestinal diseases such as inflammatory bowel disease (IBD). To understand the molecular bases, we analyzed the enterohepatic regulation of Fgf15-mediated pathway in 2 different inflammatory bowel disease mouse models.

Methods: Target genes of the BA-farnesoid-X-receptor (Fxr)-Ffg15 axis were quantified by RT-PCR or western blotting in gut and liver of dextran sulfate sodium (DSS)-treated and *IL10*$^{(-/-)}$ mice. Serum Fgf15 levels were analyzed by ELISA. Biliary and fecal BA composition was differentiated by HPLC-MS/MS.

Results: Dextran sulfate sodium-treated mice with ileum-sparing colitis showed higher Fgf15 serum levels. In contrast, *IL10*$^{(-/-)}$ mice with ileitis had a trend toward decreased Fgf15 serum levels compared with controls and increased expression of *Asbt* as a negative Fxr-target gene. In hepatic tissue of both models, no histological changes, but higher interleukin 6 (IL-6) mRNA expression and down-regulation of Fxr and Cytochrom P450 7a1 mRNA expression were observed. Fibroblast growth factor receptor 4 up-regulation was in line with higher Fgf15 serum levels in dextran sulfate sodium-treated mice. A distinct fecal BA profile was observed in both models with significantly higher levels of taurine-conjugated BA in particular tauro-β-muricholic acid in *IL10*$^{(-/-)}$ mice.

Conclusions: Ileum-sparing colitis is characterized by activation of Fxr-Fgf15 signaling with higher expression of Fxr-target gene *Fgf15*, whereas ileal inflammation showed no signs of Fxr-Fgf15 activation. Abundance of BA such as T-β-MCA may be important for intestinal Fxr activation in mice.

(Inflamm Bowel Dis 2016;22:2382–2389)

Key Words: DSS colitis, *IL10*$^{(-/-)}$ mice, Fxr, intestinal inflammation, T-β-MCA

Enterohepatic fibroblast growth factor (FGF19) in humans and Fgf15 in rodents is part of the gut-liver signaling axis and regulates bile acid (BA), glucose and lipid homeostasis, and metabolism in different physiological and pathological conditions.[1] Fibroblast growth factor (FGF) 15/19 is secreted from the enterocyte into the portal circulation, reaches the liver as major target organ, and binds to hepatic fibroblast growth factor receptor 4 (Fgfr4).[2] Ligand-receptor affinity of FGF15/19 and Fgfr4 is furthermore increased by the single-pass transmembrane protein β-Klotho, which is abundantly expressed in liver tissue.[3] Enterohepatic feedback regulation of BA homeostasis is coordinated by FGF15/19-mediated activation of FGFR4, a receptor tyrosine kinase specific for FGF15/19 in the liver and contributes to down-regulation of cytochrome P450 isoform 7A1 (CYP7A1) as the rate-limiting enzyme for BA synthesis.[4,5] Independent of this enterohepatic FGF15/19 signaling, hepatic farnesoid X receptor (FXR) activation per se inhibits CYP7A1 expression and thus BA synthesis via up-regulation of small heterodimer partner (SHP).[6,7] At the level of gall bladder motility, FGF15/19 exerts further negative feedback resulting in inhibition of bile release and hence decreasing the amount on BAs reaching the duodenum.[8]

Enterohepatic circulation of BAs contributes to the maintenance of the body BA pool.[9] In the ileum, BAs are reabsorbed by the apical Na^+-dependent BA transporter (ASBT) that is negatively feedback regulated by BAs.[10] In mice, Fxr activation by

Supplemental digital content is available for this article. Direct URL citations appear in the printed text and are provided in the HTML and PDF versions of this article on the journal's Web site (www.ibdjournal.org).

Received for publication April 6, 2016; Accepted May 12, 2016.

From the *Division of Hepatology, Department of Medicine II, University Hospital Würzburg, Würzburg, Germany; †Department of Clinical Pharmacology and Toxicology, USZ, Zurich, Switzerland; ‡Laboratory of Experimental Hepatology and Drug Targeting (HEVEFARM), IBSAL, CIBERehd, University of Salamanca, Salamanca, Spain; and §Division of Gastroenterology and Hepatology, USZ, Zurich, Switzerland.

Supported by Else-Kröner-Fresenius Stiftung 2014-A67 (to A. Geier).

The authors have no conflict of interest to disclose.

Address correspondence to: Andreas Geier, MD, Division of Hepatology, Department of Internal Medicine II, University Hospital Würzburg, Oberdürrbacherstrasse 6, D-97080 Würzburg, Germany (e-mail: geier_a2@ukw.de).

DOI 10.1097/MIB.0000000000000879

Published online 30 August 2016.

BAs in the enterocyte induces transcription of intestinal BA binding protein (Ibabp) and Fgf15.[4,11]

The gut-liver axis is in the focus of recent research of intestinal and hepatic diseases particularly in diseases affecting both organs such as inflammatory bowel disease (IBD). IBD patients have a higher prevalence of cholestatic liver diseases such as primary sclerosing cholangitis (PSC) affecting intrahepatic and extrahepatic bile ducts. In two-thirds of patients, primary sclerosing cholangitis is associated with IBD mainly ulcerative colitis (UC).[12] The etiology is still poorly understood and there are no mechanistic explanations for the strong association between primary sclerosing cholangitis and IBD to date.

Dextran sulfate sodium (DSS)-induced colitis is a well-accepted and frequently used mouse model for IBD.[13] Location and degree of colitis in DSS-treated mice is dependent on different factors, such as quantity and molecular weight of DSS, duration of administration, and the mouse strain.[14] Typically, inflammation is limited to the large intestine with minor alterations in the small bowel. In contrast, knockout mouse for interleukin 10 (*IL10*$^{(-/-)}$), which is another well-established IBD model, develops a continuously increasing inflammation in the entire gastrointestinal tract including the ileum.[15]

In our study, DSS-treated mice were investigated as a model for pancolitis without affection the terminal ileum as frequently observed in UC. *IL10*$^{(-/-)}$ mice was used as an additional IBD model with an inflammation affecting the entire gastrointestinal tract including the terminal ileum, which shares this characteristic with Crohn's disease (CD).

Because the overall functional effect of IBD on intestinal FGF19 expression, hepatic FGFR4 signaling and BA homeostasis are unknown to date, the present study aimed to analyze qualitative changes in the fecal BA profile, the enterohepatic Fgf15/Fgfr4 signaling pathway, and the potential consequences on BA pool composition in 2 different mouse models of IBD.

METHODS

Animals

C57-BL/6J-Fue female mice were housed according to the Swiss animal protection ordinance and approved by the cantonal veterinary office in the University Hospital Zurich animal facility and the local ethics committee. Access to drinking water was ad libitum. Twelve mice (age 6–8 wk) were treated with 2% dextran sulfate sodium (DSS; molecular weight 35,000–50,000) for 7 days in the drinking water. Twelve mice in the control group (age 6–8 wk) received normal drinking water for the same duration. Liver tissue, small and large bowel, and serum and bile samples were harvested together with stool samples at day 7 in the morning (2–4 hr after the last meal) and immediately stored in liquid nitrogen.

BL6-IL10tmlCgn (*IL10*$^{(-/-)}$) male mice (n = 12) were bred in the University Hospital Zurich animal facility after approval by the local ethics committees and had access to drinking water ad libitum. Animals were sacrificed after 6 to 12 months after signs of inflammation in the gastrointestinal tract in form of rectal prolapse became apparent.

Histology and Endoscopic Examination

Intestinal and hepatic tissue was immediately embedded in paraffin and fixed in 4% formalin. Sections of 3 μm were cut and stained with hematoxylin and eosin according to standard protocol. Colonic and ileal sections were analyzed accordingly. Endoscopy of the large bowel was performed as previously described.[16]

RNA Extraction and Reverse Transcription PCR

Total RNA was isolated from liver tissue and the ileum by using RNeasy Mini Kit (Qiagen, Valencia, CA) according to the manufacturer's instructions. mRNA was reverse-transcribed using the High Capacity cDNA Reverse Transcription Kit (Applied Biosystems, Mannheim, Germany). Expression was normalized against Hprt. Genes were analyzed by quantitative real-time PCR with Fast SYBR Green Master Mix (Applied Biosystems) on an Applied Biosystems 7900HT RT-PCR System. Primers were designed by using Primer express 3.0 (Applied Biosystems) and synthesized by MicroSynth AG (Balgach, Switzerland). Primers were used as previously published.[17]

Western Blot Analysis

Microsomal protein fractions were prepared from frozen liver tissue. Protein samples were separated by SDS-PAGE and blotted on nitrocellulose membranes. Antibody staining and immune complexes detection were performed as previously described.[17] Primary antibodies used in the study were directed against basolateral Na^+-dependent taurocholate cotransporting polypeptide (mNTCP[18]), multidrug-resistance-associated protein 2 (mMRP2[19]), bile salt export pump (BSEP[20]), multidrug-resistance-associated protein 4 (mMRP4) (ab45602), and multidrug-resistance-associated protein 3 (mMRP3) (ab3375). Na/K-ATPase (ab7671-50) was used as a loading control. Densitometric quantification of western blots was performed using Adobe Photoshop CS3.

Serum Analysis

Alanin-aminotransferase and bilirubin levels were measured in serum using a multiple biochemistry analyzer (Ektachem DTSCII; Johnson & Johnson Inc., Rochester, NY). Serum fibroblast growth factor 15 was quantified by ELISA Kit (E80154Mu; Uscn Life Science, Wuhan, China).

Biliary and Fecal Bile Analysis by HPLC-MS/MS Method

Bile and feces were collected during sacrifice. BAs in bile were analyzed after dilution with methanol, without further treatment. For fecal BA isolation, feces were solubilized in 50% tert-butanol and incubated over night at 4°C. After sonication at maximal power for 1 minute, samples were centrifuged. Extracted BAs were subsequently analyzed as described above.

BAs were analyzed in an HPLC-MS/MS (6410 Triple Quad LC/MS; Agilent Technologies, Santa Clara, CA) as previously reported.[21]

Statistical Analysis

Statistical significance was determined by Mann–Whitney U test. *P*-values <0.05 were considered as statistically significant (*<0.05, **<0.01, ***<0.001). Data represent the mean ± SEM. Analyzes were performed with PASW Statistics 18.0.0, (Chicago, IL) and GraphPad 5.01 (GraphPad Software Inc., CA).

RESULTS

DSS Treatment and IL-10 Deficiency Lead to Different Inflammatory Phenotypes in the Intestine Without Histological and Biochemical Alterations of the Liver

DSS-treated mice showed inflammation in the entire colon as demonstrated by colonoscopy and microscopic changes in histology (Fig. 1A). DSS treatment caused a loss of crypt structure and extensive infiltration reaching the lamina muscularis mucosae and thickening of the mucosa with abundant edema in the colon. Histological analysis of *IL10*$^{(-/-)}$ mice revealed overt inflammatory changes in colon and in the ileum (Fig. 1A, B). Histological score for inflammation and epithelial cell damage of the colon was assessed as described previously.[22] DSS-treated mice and *IL10*$^{(-/-)}$ mice had significantly increased histological score compared with the control group with the highest score in the DSS group (see Fig. 1, Supplemental Digital Content 1, http://links.lww.com/IBD/B315). Murine endoscopic index of colitis severity (MEICS) was significantly increased in DSS-treated mice. DSS-treated mice further showed a significant shortening of the colon (mean ± SEM: 6.4 ± 0.1 cm [DSS] versus 9.0 ± 0.2 cm [control]; $P < 0.0001$) and weight loss (mean ± SEM: −7.6 ± 1.3% [DSS] versus 3.0 ± 1.0% [control]; $P < 0.0001$) at the end of the DSS treatment. In the control group, no colonic epithelial damage or infiltration was found.

In both IBD mice models, gene expression in the ileum of tumor necrosis factor-α (TNF-α) was investigated to better characterize the site of inflammation. In DSS-treated mice, the primary inflammatory site was limited to the colon, confirmed by reduced TNF-α expression in ileum compared with control. In contrast, *IL10*$^{(-/-)}$ showed higher ileal TNF-α gene expression, which is in line with inflammatory changes affecting also the small intestine (Fig. 1C).

No histological changes in the liver have been observed in both DSS-treated and *IL10*$^{(-/-)}$ mice (Fig. 2). Liver function tests in serum including alanin-aminotransferase, bilirubin, and BAs were not elevated in DSS-treated mice (data not shown).

The Fxr-Fgf15 Pathway Is Differentially Regulated in the Ileum of DSS-treated and *IL10*$^{(-/-)}$ Mice

Functional consequences of intestinal inflammation on the Fxr-Fgf15 pathway in the ileum, which is mainly involved in BA signaling and absorption, were analyzed. Fgf15 mRNA expression and Fgf15 protein levels in serum were analyzed in both mouse models. mRNA expression of ileal Fgf15 and Fgf15 protein in serum were increased in DSS-treated mice compared with controls (mRNA mean ± SEM: 256.3 ± 55% of control, $P < 0.05$; protein mean ± SEM: 622.8 ± 119.7 pg/ml [DSS] versus 368.6 ± 46.8 mg/dL [control], $P < 0.05$). On mRNA level, no changes were observed for *IL10*$^{(-/-)}$ mice, but significantly lower Fgf15 serum levels were measured (222.1 ± 27.9 pg/ml [*IL10*$^{(-/-)}$] versus 622.8 ± 119.7

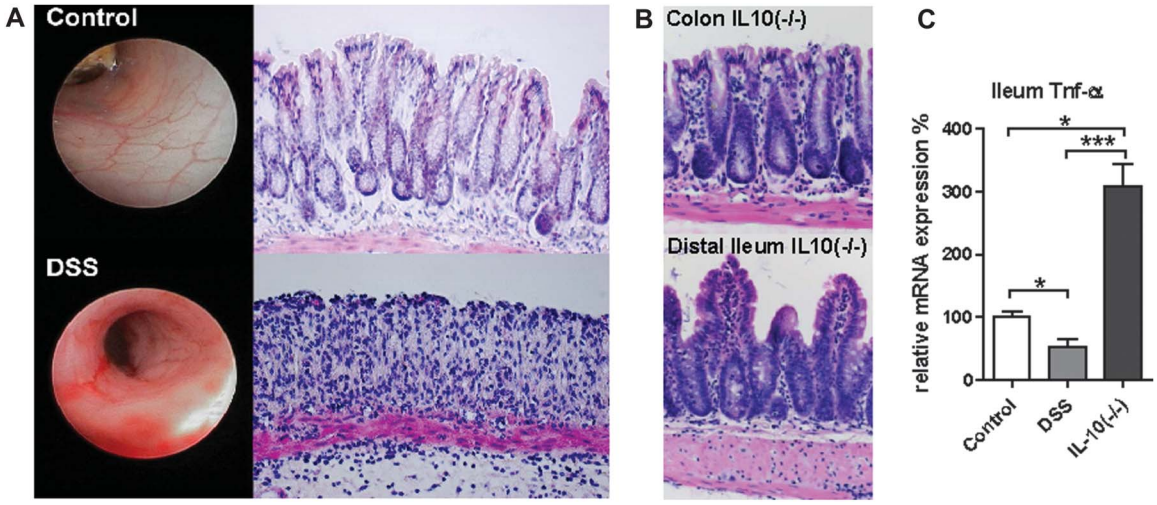

FIGURE 1. Endoscopic images and histological findings in DSS and *IL10*$^{(-/-)}$ mice. A, Representative images of colonoscopy and histology in control mice without signs of inflammation and DSS-treated mice with macroscopic and microscopic signs of colitis. B, Colonic and ileal histology of *IL10*$^{(-/-)}$ mice with signs of inflammation. C, Relative mRNA expression of TNF-α in ileum of control mice, DSS-treated mice, and *IL10*$^{(-/-)}$ mice with highest TNF-α expression in *IL10*$^{(-/-)}$ mice. *$P < 0.05$, **$P < 0.01$, ***$P < 0.001$.

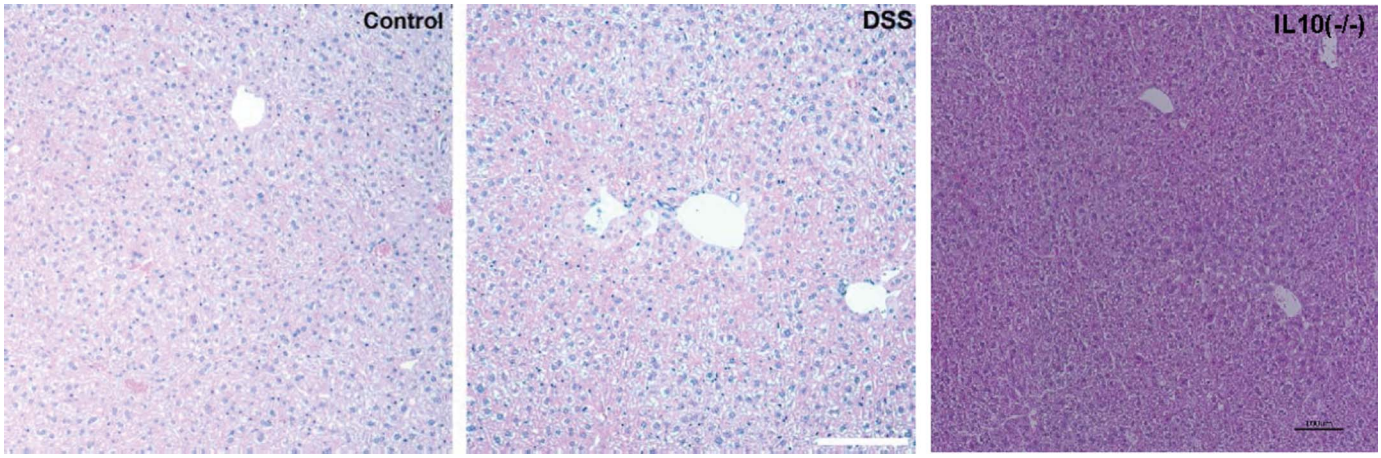

FIGURE 2. Liver histology in DSS and *IL10*$^{(-/-)}$ mice. Microscopic no pathologic findings in control, DSS, and *IL10*$^{(-/-)}$ were observed.

pg/ml [DSS], $P < 0.05$) compared with DSS-treated mice and a trend toward lower Fgf15 serum levels was observed even in comparison with WT mice (Fig. 3A, B).

These findings suggested that intestinal inflammation not including the ileum as observed in DSS-treated mice leads to activation of Fxr-Fgf15 pathway, which is absent in *IL10*$^{(-/-)}$ mice. Therefore, expression of further Fxr target genes was analyzed in DSS-treated mice. In line with Fxr activation, no up-regulation of the negative Fxr target gene *Asbt* was observed in DSS mice, whereas higher expression of Asbt was seen in *IL10*$^{(-/-)}$ mice (Fig. 3C).

Intestinal Inflammation Leads to a Down-regulation of Hepatic Cyp7a1 and BA Transporter Genes

Interleukin 6 (IL-6) mRNA as a proinflammatory cytokine was significantly elevated in the liver of DSS-treated and *IL10*$^{(-/-)}$ mice (mean ± SEM: 324.8 ± 99.8% [DSS] of controls; $P < 0.05$ and 463.5 ± 67.1% [*IL10*$^{(-/-)}$] of controls; $P < 0.01$), indicating inflammatory changes at the molecular level despite the absence of macroscopic and microscopic changes (Fig. 4A). Expression of Fgfr4 mRNA was increased in DSS-treated mice (133.8 ± 18.2% of controls, $P < 0.05$) and decreased in *IL10*$^{(-/-)}$ mice (52.7 ± 7.3% of controls, $P < 0.01$) (Fig. 4B). These changes are in line with differences in Fgf15 serum levels in these mouse models.

Quantification of BA target genes in hepatic tissue showed no significant change of Fxr expression in DSS-treated mice (84.9 ± 11.1% of controls), but down-regulation of the rate-limiting enzyme for BA synthesis, that is, Cyp7a1 (42.4 ± 14.9% of controls, $P < 0.05$), which is well in accordance with the observed increase in Fgf15 and Fgfr4 expression. In *IL10*$^{(-/-)}$ mice, a decreased Fxr expression (64.0 ± 8.0% of controls, $P < 0.001$) and a reduction in Cyp7a1 mRNA levels (32.7 ± 4.2% of controls, $P < 0.001$) in liver were observed (Fig. 4C, D).

Expression of genes involved in BA transport by hepatocytes was mostly decreased in both mouse models as shown in Fig. 2,

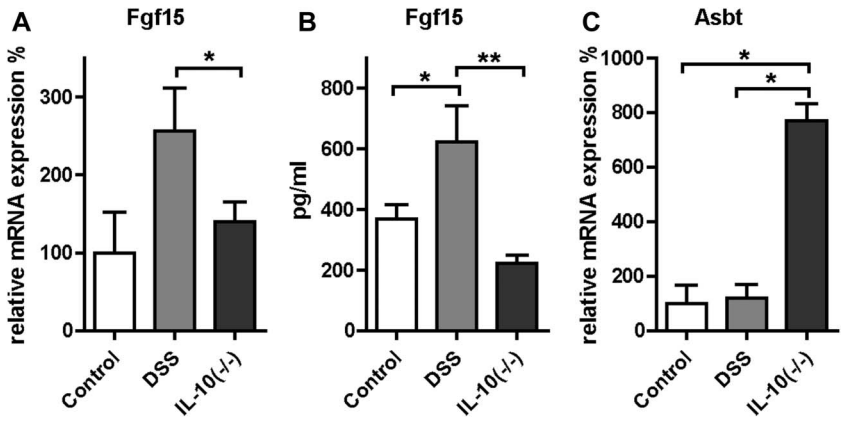

FIGURE 3. Relative mRNA expression of target genes in ileum and Fgf15 serum levels. A, Significant higher Fgf15 mRNA expression was observed in DSS-treated mice in comparison with *IL10*$^{(-/-)}$ mice. B, Ffg15 serum levels were significantly increased in DSS-treated mice compared with control and *IL10*$^{(-/-)}$ mice. C, Asbt mRNA expression was significantly increased in *IL10*$^{(-/-)}$ mice and no change was observed for DSS mice compared with control mice. *$P < 0.05$, **$P < 0.01$, ***$P < 0.001$.

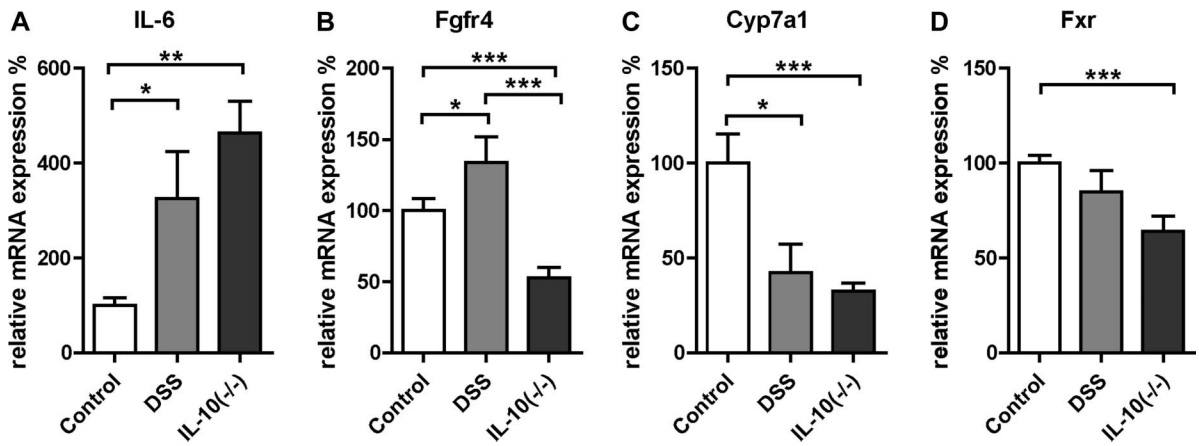

FIGURE 4. Hepatic target genes of bile acid metabolism. A–D, Relative mRNA expression of IL-6, Fgfr4, Cyp7a1 and Fxr in control, DSS-treated mice, and *IL10*$^{(-/-)}$ mice. *$P < 0.05$, **$P < 0.01$, ***$P < 0.001$.

Supplemental Digital Content 2, http://links.lww.com/IBD/B316. Ntcp mRNA expression, as a principal BA transporter, was significantly lower in DSS-treated and *IL10*$^{(-/-)}$ mice (Ntcp: 60.6 ± 7.4% [DSS] and 51.7 ± 7.1% [*IL10*$^{(-/-)}$] of controls, $P < 0.01$ and $P < 0.001$). Bsep mRNA expression was significantly reduced in DSS-treated mice and a trend toward decreased Bsep expression was observed in *IL10*$^{(-/-)}$ mice (Bsep: 69.7 ± 9.5% [DSS] and 77.2 ± 8.0% [*IL10*$^{(-/-)}$] of controls, $P < 0.01$ and $P < 0.001$). Changes on mRNA level were confirmed by similar findings for protein expression in western blotting in DSS-treated mice (see Fig. 3, Supplemental Digital Content 3, http://links.lww.com/IBD/B317).

Qualitative Changes in Biliary BA Profile in DSS Mice and *IL10*$^{(-/-)}$ Mice

To investigate whether these changes in genes involved in BA homeostasis lead to changes in the composition of murine bile

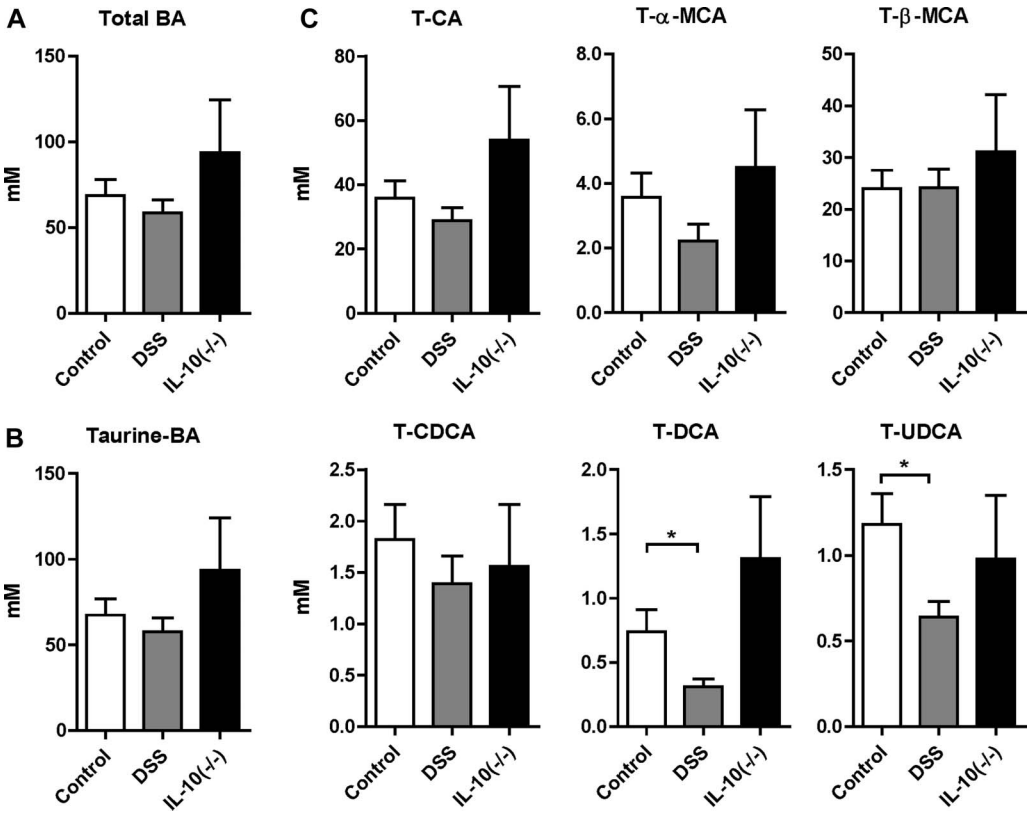

FIGURE 5. Changes in biliary bile acids profile. A–E, Biliary concentrations of total BAs and taurine-conjugated BAs in different mice models are depicted. *$P < 0.05$, **$P < 0.01$, ***$P < 0.001$.

concentrations of total BAs, unconjugated BAs and glycine or taurine-conjugated BAs were determined. In agreement with previously described results by Jahnel et al[23] for DSS mice, no significant change in total BA concentration in gallbladder bile of DSS-treated mice (58.4 ± 7.6 mM) and *IL10*$^{(-/-)}$ mice (93.7 ± 30.8 mM) versus control mice (68.6 ± 9.4 mM) was detected (Fig. 5A). Murine BAs are predominantly conjugated with taurine. In DSS-treated animals, qualitative changes in taurine-conjugated BA showed a decrease in taurine conjugates such as tauroursodeoxycholic acid (T-UDCA) (1.18 ± 0.18 mM [control] versus 0.64 ± 0.09 mM [DSS]) and taurodeoxycholic acid (T-DCA) (0.74 ± 0.17 [control] versus 0.31 ± 0.06 mM [DSS], $P < 0.05$ each). No significant difference was observed in taurine-conjugated BAs for *IL10*$^{(-/-)}$ mice (Fig. 5B, C).

Only low levels of glycocholic acid as a glycine-conjugated BA were measured with a decrease in DSS-treated and *IL10*$^{(-/-)}$ mice (0.03 ± 0.01 mM [DSS], 0.02 ± 0.01 mM [*IL10*$^{(-/-)}$] versus 0.06 ± 0.01 mM [control]) (see Fig. 4A, Supplemental Digital Content 4, http://links.lww.com/IBD/B318). Unconjugated BAs showed a trend to decreased concentrations in DSS-treated and *IL10*$^{(-/-)}$ mice (see Fig. 4B, Supplemental Digital Content 4, http://links.lww.com/IBD/B318). Analysis of qualitative changes of free BAs showed significantly decreased α- and β-muricholic acid (M-CA) (as naturally hydrophilic and therefore less cytotoxic BAs) in the bile of DSS-treated mice (0.31 ± 0.17 mM versus 0.17 ± 0.08 mM and 0.17 ± 0.08 mM versus 0.03 ± 0.01 mM, respectively; $P < 0.05$ each). *IL10*$^{(-/-)}$ mice showed a trend toward decreased α-, β-MCA and cholic acid (CA) (see Fig. 4C–E, Supplemental Digital Content 4, http://links.lww.com/IBD/B318).

DSS-Treated and *IL10*$^{(-/-)}$ Mice Have Distinct Fecal BA Profiles

Fecal BA composition as an established effector of intestinal Fxr/Fgf15 activation was characterized in the same detail. Interestingly, DSS-treated mice showed changes with a trend toward decreased total BAs, unconjugated BA, and significant changes in primary (CA and chenodeoxycholic acid [CDCA]) and secondary BAs such as deoxycholic acid (DCA) and litocholic acid (LCA) (not significant) (Fig. 6A; see Fig. 5B, Supplemental Digital Content 5, http://links.lww.com/IBD/B319). No major changes were seen in taurine-conjugated BAs (Fig. 6B). *IL10*$^{(-/-)}$ mice showed a significant reduction of total and unconjugated BAs. Free α-MCA, CDCA, ursodeoxycholic acid (UDCA), Hyo-DCA, LCA, and DCA were significantly reduced in *IL10*$^{(-/-)}$ mice in contrast to β-muricholic acid, which was significantly increased (Fig. 6A; see Fig. 5A, B, Supplemental Digital Content 5, http://links.lww.com/IBD/B319). Interestingly, total taurine-conjugated BAs were significantly increased in *IL10*$^{(-/-)}$ mice with the highest increase in tauro-β-MCA (T-β-MCA), T-UDCA, T-CDCA, T-DCA, and T-CA (Fig. 6B; see Fig. 5A, B, Supplemental Digital Content 5, http://links.lww.com/IBD/B319).

DISCUSSION

Enterohepatic FGF15/19 signaling is an important pathway for the regulation of BA metabolism between gut and liver. Although recent studies have described altered FGF19 serum levels in patients with IBD, neither the underlying regulatory events nor the pathophysiological contribution of FGF19 signaling to biliary pathophysiology had been elucidated. To get further mechanistic insight, we put focus on the analysis of the murine orthologue of FGF19, that is, Fgf15 signaling and biliary and fecal BA profile in 2 different IBD mouse models with different sites of inflammation.

Two recent studies showed slightly increased[24] or rather unchanged[25] FGF19 serum concentrations in patients with UC in comparison with healthy controls. Interestingly, however, the same studies consistently showed that patients with CD had significantly lower levels of FGF19 in serum. Patients with the history of ileal resection had the lowest levels of FGF19 in serum. This is consistent with the established concept that FGF19 is mainly expressed in the distal ileum.

In both human studies, serum changes of FGF19 have been analyzed together with the inflammatory site pattern. In this regard, Lenicek et al[25] reported that FGF19 down-regulation only appeared in cases with a significant ileal involvement because CD patients with Crohn's colitis had normal FGF19 serum levels and only those with ileitis had significantly decreased FGF19 levels compared with controls. Consistently, in the study of Iwamoto et al,[24] the only patient with CD and a colonic inflammation had higher FGF19 levels than other CD patients.

In our study, the data derived from 2 different mouse models show well comparable changes in serum Fgf15 levels: While DSS-treated mice—as a model of pancolonic inflammation sparing the ileum—had increased Fgf15 mRNA and serum protein levels, serum Fgf15 tended to be decreased in *IL10*$^{(-/-)}$ mice that rather resemble human patients with CD due to the presence of ileal inflammation. In this regard, Fgf15 expression in both our mouse models nicely reflects FGF19 expression in the human clinical situation. Our findings therefore strengthen the usefulness of these mouse models to investigate the significance of FGF15/FGF19 signaling for the pathophysiology of human IBD.

Another clinical study in humans analyzed FXR mRNA levels in the ileum of patients with UC and CD without significant differences at the message level, but interestingly a lower expression of SHP (as a direct transcriptional target of FXR) was observed in patients with CD.[26] The authors concluded that FXR activity may be decreased in this subtype of IBD but did not find any association of genetic variation in *FXR* gene and IBD as the primary objective of their study.[26] In our study, Fgf15 signaling was activated in DSS-treated mice with a primary inflammatory site in the colon. In contrast, *IL10*$^{(-/-)}$ mice with inflammatory changes in the complete gastrointestinal tract and also in ileum had a trend toward lower Fgf15 serum levels, suggesting a putative moderate decrease of *Fxr* transactivation activity in this group. Based on our results and the data derived from the clinical studies cited above, it

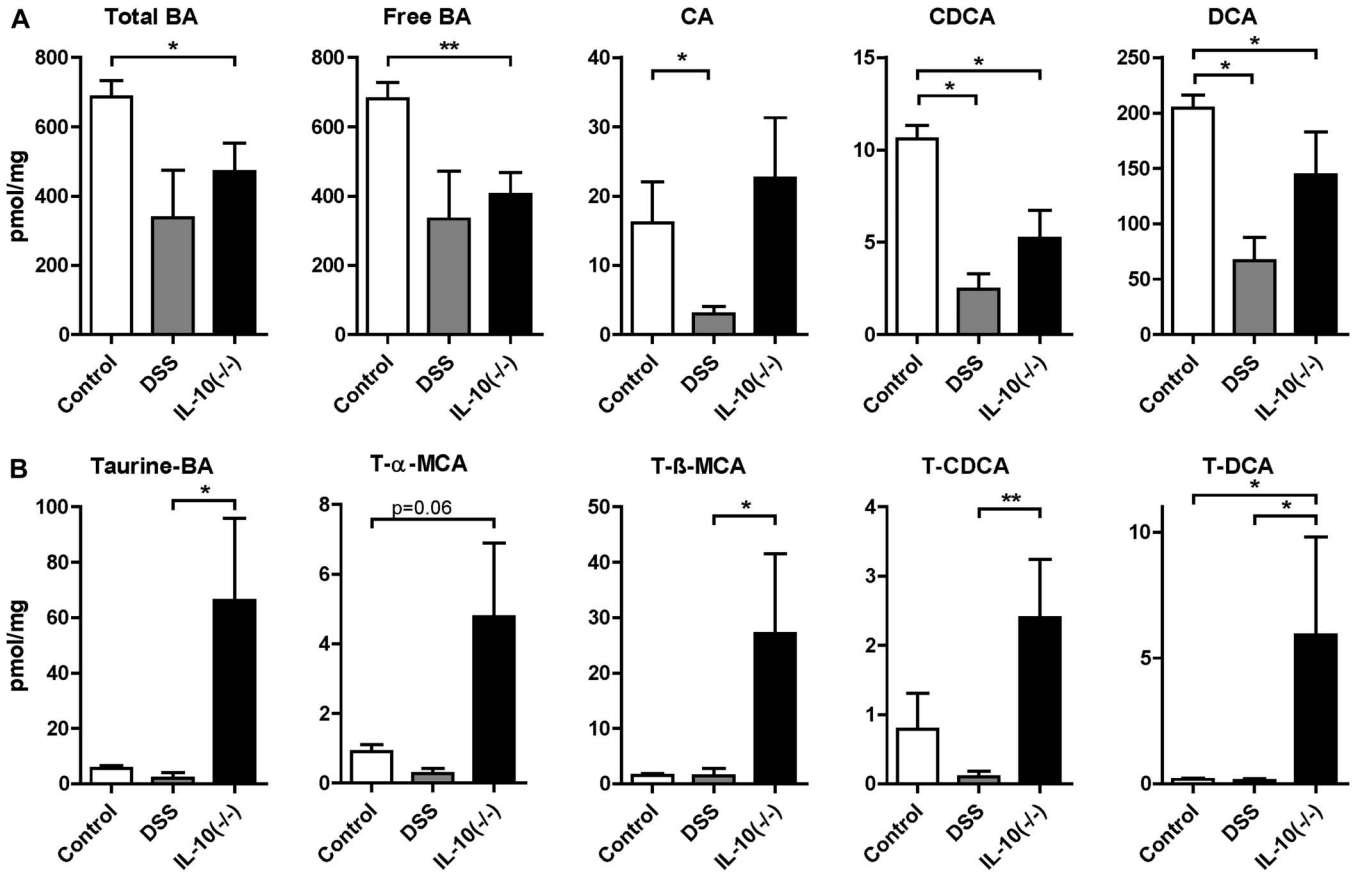

FIGURE 6. Fecal bile acids profile in mice. A, Changes in total BAs, free Bas, and primary and secondary BAs such as CA, CDCA, and DCA in control, DSS, and *IL10*$^{(-/-)}$ mice. B, Taurine-conjugated BAs in the 3 mice groups. *$P < 0.05$, **$P < 0.01$, ***$P < 0.001$.

can be hypothesized that ileitis in humans with CD and in *IL10*$^{(-/-)}$ mice is consistently characterized by decreased *Fxr* transactivation ability that modulates the expression of several Fxr-target genes including Fgf15.

An interesting question arises with regard to the molecular mechanism accounting for the alterations observed in the intestinal Fxr-Fgf15 axis under conditions of ileal inflammation. A recent study has suggested that the gut microbiota plays a crucial role for the regulation of Fgf15 signaling. Sayin et al[27] showed important changes in fecal biliary profile in germ-free mice. Conventional mice in comparison with germ-free mice showed an up-regulated expression of Fxr and its target genes (including Fgf15) in the distal ileum but not in the liver. Taurine-conjugated α- and β-MCA were identified as strong Fxr antagonist in this study with suppressive function of T-β-MCA on T-CA (Fxr agonist)-treated ileal explants from conventional mice. Interestingly, germ-free mice showed higher concentrations of T-β-MCA and T-CA in comparison with conventional mice defining a molecular basis for the altered expression of gut-specific Fxr targets in that study.

With regard to this concept, it is an intriguing finding of our study that *IL10*$^{(-/-)}$ mice are characterized by a significant increase in T-β-MCA in feces. Furthermore, as already described above, lower Fgf15 serum levels (as well as increased expression of Asbt as a negative Fxr target gene) were observed in these mice in comparison with DSS-treated mice. In contrast, DSS-treated mice had no significant changes in fecal T-β-MCA in comparison with control mice. Together with the data provided by Sayin et al, our results therefore suggest that one mechanism that contributes to the pronounced changes of Fxr target gene expression (including Fgf15) in the IBD mouse models could rely on the altered abundance of the potent Fxr antagonists T-α-MCA and T-β-MCA in the intestine.

In both murine IBD models used in the present study, no macroscopic changes in liver histology were observed, but an increase of IL-6 mRNA expression as an indicator of molecular hepatic inflammation with reduced mRNA expression of several BAs transporters and Cyp7a1 has been detected. This finding is well in line with the fact that treatment with recombinant Tnf-α, IL1-β, or IL-6 in C57BL/6 mice showed a transient or sustained down-regulation of different hepatic BA transporters such as Ntcp and Bsep[6,28] and Cyp7a1.[29] Furthermore, cytokine treatment had effects on mRNA expression of transcription factors with reduced Fxr expression after Tnf-α treatment.[30] In a recent study, Jahnel et al[23] analyzed hepatic tissue of DSS-treated mice (male BL6 mice received 3% DSS for 7 d) and did not observe any

functionally relevant changes in hepatocyte gene expression (e.g., Cyp7a1, Ntcp, Bsep, Fxr) and bile composition. In contrast to our study, no change for mRNA expression of inflammatory cytokines such as Tnf-α could be observed. Of note, our findings are not in contradiction to the study of Jahnel et al[23] where no signs of inflammation were found in hepatic tissue of mice using a different DSS-treatment protocol.

As a hypothesis-building finding, our study firstly describes an inverse regulation of Fgf15 signaling in IBD mouse models according to the distinct sites of intestinal inflammation. Transactivation of this pathway was observed in DSS-treated mice without ileal inflammation. In contrast, *IL10*$^{(-/-)}$ mice with present ileitis but absent induction of intestinal Fxr target genes exhibited significant changes in fecal BA profile together with high levels of T-β-MCA as a strong Fxr antagonist. These fuel the hypothesis that both local inflammatory signals and alterations in fecal BA composition could be an important regulator of the enterohepatic Fxr-/Fgf15 axis under intestinal inflammation. Whether the observed changes contribute to the development of cholestatic liver disease in patients with certain site patterns of inflammatory bowel disease remains to be investigated in subsequent studies.

REFERENCES

1. Jahn D, Rau M, Hermanns HM, et al. Mechanisms of enterohepatic fibroblast growth factor (FGF) 15/19 signaling in health and disease. *Cytokine Growth Factor Rev.* 2015;26:625–635.
2. Beenken A, Mohammadi M. The FGF family: biology, pathophysiology and therapy. *Nat Rev Drug Discov.* 2009;8:235–253.
3. Fon Tacer K, Bookout AL, Ding X, et al. Research resource: Comprehensive expression atlas of the fibroblast growth factor system in adult mouse. *Mol Endocrinol.* 2010;10:2050–2064.
4. Inagaki T, Choi M, Moschetta A, et al. Fibroblast growth factor 15 functions as an enterohepatic signal to regulate bile acid homeostasis. *Cell Metab.* 2005;2:217–225.
5. Holt JA, Luo G, Billin AN, et al. Definition of a novel growth factor-dependent signal cascade for the suppression of bile acid biosynthesis. *Genes Dev.* 2003;17:1581–1591.
6. Goodwin B, Jones SA, Price RR, et al. A regulatory cascade of the nuclear receptors FXR, SHP-1, and LRH-1 represses bile acid biosynthesis. *Mol Cell.* 2000;6:517–526.
7. Lu TT, Makishima M, Repa JJ, et al. Molecular basis for feedback regulation of bile acid synthesis by nuclear receptors. *Mol Cell.* 2000;6:507–515.
8. Houten SM. Homing in on bile acid physiology. *Cell Metab.* 2006;4:423–424.
9. Gadaleta RM, van Mil SW, Oldenburg B, et al. Bile acids and their nuclear receptor FXR: relevance for hepatobiliary and gastrointestinal disease. *Biochim Biophys Acta.* 2010;1801:683–692.
10. Kullak-Ublick GA, Stieger B, Meier PJ. Enterohepatic bile salt transporters in normal physiology and liver disease. *Gastroenterology*. 2004;126:322–342.
11. Inagaki T, Moschetta A, Lee YK, et al. Regulation of antibacterial defense in the small intestine by the nuclear bile acid receptor. *Proc Natl Acad Sci U S A.* 2006;103:3920–3925.
12. Maggs JR, Chapman RW. An update on primary sclerosing cholangitis. *Curr Opin Gastroenterol.* 2008;24:377–383.
13. Okayasu I, Hatakeyama S, Yamada M, et al. A novel method in the induction of reliable experimental acute and chronic ulcerative colitis in mice. *Gastroenterology*. 1990;98:694–702.
14. Mahler M, Bristol IJ, Leiter EH, et al. Differential susceptibility of inbred mouse strains to dextran sulfate sodium-induced colitis. *Am J Physiol.* 1998;274:G544–G551.
15. Kuhn R, Lohler J, Rennick D, et al. Interleukin-10-deficient mice develop chronic enterocolitis. *Cell*. 1993;75:263–274.
16. Leucht K, Caj M, Fried M, et al. Impaired removal of Vbeta8(+) lymphocytes aggravates colitis in mice deficient for B cell lymphoma-2-interacting mediator of cell death (Bim). *Clin Exp Immunol.* 2013;173:493–501.
17. Martin IV, Schmitt J, Minkenberg A, et al. Bile acid retention and activation of endogenous hepatic farnesoid-X-receptor in the pathogenesis of fatty liver disease in ob/ob-mice. *Biol Chem.* 2010;391:1441–1449.
18. Stieger B, Hagenbuch B, Landmann L, et al. In situ localization of the hepatocytic Na+/Taurocholate cotransporting polypeptide in rat liver. *Gastroenterology*. 1994;107:1781–1787.
19. Madon J, Hagenbuch B, Landmann L, et al. Transport function and hepatocellular localization of mrp6 in rat liver. *Mol Pharmacol.* 2000;57:634–641.
20. Gerloff T, Stieger B, Hagenbuch B, et al. The sister of P-glycoprotein represents the canalicular bile salt export pump of mammalian liver. *J Biol Chem.* 1998;273:10046–10050.
21. Nytofte NS, Serrano MA, Monte MJ, et al. A homozygous nonsense mutation (c.214C->A) in the biliverdin reductase alpha gene (BLVRA) results in accumulation of biliverdin during episodes of cholestasis. *J Med Genet.* 2011;48:219–225.
22. Obermeier F, Kojouharoff G, Hans W, et al. Interferon-gamma (IFN-gamma) and tumor necrosis factor (TNF)-induced nitric oxide as toxic effector molecule in chronic DSS-induced colitis in mice. *Clin Exp Immunol.* 1999;116:238–245.
23. Jahnel J, Fickert P, Langner C, et al. Impact of experimental colitis on hepatobiliary transporter expression and bile duct injury in mice. *Liver Int.* 2009;29:1316–1325.
24. Iwamoto J, Saito Y, Honda A, et al. Bile acid malabsorption deactivates pregnane X receptor in patients with Crohn's disease. *Inflamm Bowel Dis.* 2013;19:1278–1284.
25. Lenicek M, Duricova D, Komarek V, et al. Bile acid malabsorption in inflammatory bowel disease: assessment by serum markers. *Inflamm Bowel Dis.* 2011;17:1322–1327.
26. Nijmeijer RM, Gadaleta RM, van Mil SW, et al. Farnesoid X receptor (FXR) activation and FXR genetic variation in inflammatory bowel disease. *PLoS One*. 2011;6:e23745.
27. Sayin SI, Wahlstrom A, Felin J, et al. Gut microbiota regulates bile acid metabolism by reducing the levels of tauro-beta-muricholic acid, a naturally occurring FXR antagonist. *Cell Metab.* 2013;17:225–235.
28. Siewert E, Dietrich CG, Lammert F, et al. Interleukin-6 regulates hepatic transporters during acute-phase response. *Biochem Biophys Res Commun.* 2004;322:232–238.
29. Merrell MD, Nyagode BA, Clarke JD, et al. Selective and cytokine-dependent regulation of hepatic transporters and bile acid homeostasis during infectious colitis in mice. *Drug Metab Dispos.* 2014;42:596–602.
30. Geier A, Dietrich CG, Voigt S, et al. Cytokine-dependent regulation of hepatic organic anion transporter gene transactivators in mouse liver. *Am J Physiol Gastrointest Liver Physiol.* 2005;289:G831–G841.